Activity-Dependent Calcium Sequestration in Dendrites of Hippocampal Neurons in Brain Slices

Lucas D. Pozzo-Miller,[1,2] Natalia B. Pivovarova,[1] Richard D. Leapman,[3] Roger A. Buchanan,[1] Thomas S. Reese,[1,2] and S. Brian Andrews[1,2]

[1]Laboratory of Neurobiology, National Institute of Neurological Diseases and Stroke, National Institutes of Health, Bethesda, Maryland 20892, [2]Marine Biological Laboratory, Woods Hole, Massachusetts 02543, and [3]Biomedical Engineering and Instrumentation Program, National Center for Research Resources, National Institutes of Health, Bethesda, Maryland 20892

Synaptic activity-dependent changes in the spatio-temporal distribution of calcium ions regulate important neuronal functions such as dendritic integration and synaptic plasticity, but the processes that terminate the free Ca^{2+} transients associated with these changes remain unclear. We have characterized at the electron microscopic level the intracellular compartments involved in buffering free Ca^{2+} transients in dendritic cytoplasm of CA3 neurons by measuring the larger changes in the concentrations of total Ca that persist for several minutes after neuronal activity. Quantitative energy-dispersive x-ray microanalysis of cryosections from hippocampal slice cultures rapidly frozen 3 min after afferent synaptic activity identified a subset of dendritic endoplasmic reticulum (ER) as a high-capacity Ca^{2+} buffer. Calcium sequestration by cisterns of this subset of ER was graded, reversible, and dependent on a thapsigargin-sensitive Ca^{2+}-ATPase. Sequestration was so robust that after repetitive high-frequency stimulation the Ca content of responsive ER cisterns increased as much as 20-fold. These results demonstrate that a subpopulation of ER is the major dendritic Ca sequestration compartment in the minutes after neuronal activity.

Key words: calcium regulation; calcium sequestration; hippocampus; CA3; dendrites; endoplasmic reticulum; synaptic activity; hippocampal slice cultures; X-ray microanalysis

Despite the wealth of information about the role of Ca ions in neuronal function (Miller, 1988), and especially about the channels and stores that give rise to free Ca^{2+} transients (Tsien and Tsien, 1990; Simpson et al., 1995), the processes that terminate such transients are not well understood (Miller, 1991; Pozzan et al., 1994). In particular, several important characteristics of neuronal Ca handling immediately after synaptic activity-induced cytosolic Ca^{2+} transients remain unclear, including the absolute size and fate of the underlying total Ca load. Likely candidates for clearing cytosolic Ca^{2+} include the same mechanisms that neurons employ to maintain low resting levels of intracellular free Ca^{2+}, namely, binding to cytoplasmic proteins, uptake into the smooth endoplasmic reticulum (ER) via a Ca^{2+}–ATPase (SERCA) pump, electrochemically driven uptake into mitochondria, and extrusion across the plasma membrane by the Na^{+}–Ca^{2+} exchanger and a plasma membrane Ca^{2+}–ATPase (Carafoli, 1987; Miller, 1991).

The ER has been the focus of considerable attention since the original demonstrations of its Ca-sequestering activity (Henkart et al., 1978; McGraw et al., 1980). Since then, a related but distinct Ca^{2+}-regulating function of the ER, namely, that of a releasable Ca^{2+} store, has been well characterized (Alford et al., 1993; Llano et al., 1994; Seymour-Laurent and Barish, 1995; Pozzo-Miller et al., 1996; Garaschuk et al., 1997; Golovina and Blaustein, 1997). This store, because it is engaged in cycles of Ca^{2+} uptake and release, plays an important role in neuronal Ca^{2+} buffering (Andrews et al., 1988; Markram et al., 1995). It is also now recognized, on the basis of the heterogeneous distribution of luminal Ca-binding proteins, membrane Ca^{2+}-ATPase pumps, and Ca^{2+}-permeable membrane channels, that the various functional aspects of the ER, and particularly the dendritic ER, are spatially compartmentalized (Henzi and MacDermott, 1992; Pozzan et al., 1994), even though the ER forms a structurally continuous network of membranes (Martone et al., 1993; Terasaki et al., 1994).

Direct measurements correlating neuronal activity with changes in the total Ca content of the ER would potentially reveal and localize any high-capacity sequestration activity that might function in signal termination and distinguish this from a Ca^{2+} release function. At present, such measurements are nonexistent, not only for the ER but also for other subcellular compartments of neurons. The latter is equally important, because Ca^{2+} buffering and sequestration do not reside exclusively in the ER, as indicated by the high Ca^{2+}-binding capacity of many cytoplasmic proteins (Miller, 1991) and by recent and accumulating evidence for the participation of mitochondrial Ca^{2+} uptake (Rizzuto et al., 1993; Friel and Tsien, 1994; Werth and Thayer, 1994; White and Reynolds, 1995; Budd and Nicholls, 1996; Herrington et al., 1996; Babcock et al., 1997). As a first step in establishing the roles of, as well as the interplay between, each of these mechanisms in dendritic Ca^{2+} handling, we have determined the amount and

location of intracellular Ca in proximal dendrites of CA3 pyramidal cells in hippocampal slice cultures, both at rest and at defined times after neuronal activity. These experiments were performed by exploiting the high analytical sensitivity and subcellular resolution of modern (Leapman and Andrews, 1991; Buchanan et al., 1993; Andrews et al., 1994) energy-dispersive x-ray (EDX) microanalysis (Shuman et al., 1976; Hall and Gupta, 1983), a technique that—in distinction to imaging with Ca^{2+}-sensitive fluoresecent dyes—provides direct and quantitative measurements of the concentration of total Ca within identified subcellular compartments.

MATERIALS AND METHODS

Preparation, stimulation, recording, and rapid freezing of hippocampal slice cultures. Hippocampal slice cultures were prepared from postnatal d 7 rats, as described previously (Stoppini et al., 1991; Pozzo-Miller et al., 1993). Slice cultures 6–8 d *in vitro* were transferred to an immersion chamber continuously perfused (2–4 ml/min) with artificial CSF (ACSF) at room temperature (23–24°C), containing (in mM): 124 NaCl, 2 KCl, 1.3 $MgSO_4$, 1.24 KH_2PO_4, 17.6 $NaHCO_3$, 2.5 $CaCl_2$, and 10 D-glucose, equilibrated with 95% O_2/5% CO_2. Thapsigargin (Sigma, St. Louis MO; Research Biochemicals, Natick MA; 10 μM in 0.01% DMSO) and TTX (Sigma; 5 μM) were added to the perfusion ACSF as indicated. Field EPSPs in CA3 stratum (st.) lucidum were evoked by stimulation of dentate gyrus st. granulosum or the mossy fiber track in CA3 st. lucidum with a bipolar stainless steel electrode and recorded with a ACSF-filled glass pipette (5 MΩ) using an Axoclamp-2A amplifier (Axon Instruments, Foster City, CA). Test stimuli consisting of single monophasic pulses of 100 μsec duration were delivered by a stimulus isolator–constant current unit (Axon Instruments) at an intensity of 10–100 μA at 0.25–0.5 Hz. After establishing that EPSPs were stable in the slice (0.5–2 mV; 5–15 min), high-frequency stimuli consisting of one or four trains every 30 sec, each composed of 50 pulses at 50 Hz at test intensities, were delivered to the afferent fibers. After withdrawing the recording and stimulating electrodes, slices were removed from the recording chamber, mounted on 400-μm-thick agar–gelatin pads, marked to locate cell layers for subsequent cryosectioning, and rapidly frozen by impact onto a liquid nitrogen-cooled copper block using a custom-modified CF-100 machine (LifeCell, The Woodlands, TX). The interval from the last high-frequency train in the recording chamber to the instant of freezing was 3.0 ± 0.5 min. Postsynaptic responses were digitized on-line at 10 kHz (ITC-16; Instrutech, Great Neck, NY) for display and analysis and stored on magnetic media using custom-written software in a Power PC Macintosh computer (T. Inuoe, Tokyo University, Tokyo, Japan).

Electron microscopy, cryosectioning, and quantitative EDX microanalysis. For morphological evaluation, rapidly frozen slice cultures were freeze-substituted in 4% OsO_4 in acetone at −80C° over 48 hr (Pozzo-Miller and Landis, 1993), resin-embedded (Araldite) and thin-sectioned using standard techniques, and examined in a JEOL (Peabody, MA) 100-CX electron microscope. Structural preservation in rapidly frozen slice cultures (Pozzo-Miller and Landis, 1993) varies with distance from the cryogenic contact surface. To ensure technically satisfactory preparations that showed no evidence of ice crystal-induced distortions, section depth was limited to <20 μm, at which depth rapid freezing has been calculated to occur in <2 msec (Heuser et al., 1979).

Cryosectioning was performed as described previously (Michel et al., 1992; Buchanan et al., 1993). In brief, cryosections were cut *en face* from the well frozen surface (<20 μm deep) of previously marked regions of CA3 st. lucidum, trimmed to a 0.25 × 0.25 mm block face. The *en face* orientation ensures that all material was taken from the well frozen surface and has the additional advantage that the somatic region of pyramidal cells was often contained in the margin of sections, thereby aiding the identification and location of CA3 dendrites. Cryosections were obtained as smooth, continuous ribbons at less than −160°C with a specimen advance of 80 nm using a diamond knife in an Ultracut S/FCS ultracryomicrotome (Leica, Deerfield, IL). The actual physical section thickness is approximately doubled on account of unrelievable compression, but the unidirectional nature of the compression only distorts organelle shape in the direction of knife movement; it does not increase organelle overlap relative to the original 80-nm sections (Shi et al., 1996). Therefore, such sections are suitable for elemental analysis of structures ≥80 nm in the z (thickness) direction. Sections were mounted on carbon- and Formvar-coated grids and cryotransferred into an EM912 Omega

electron microscope (LEO Electron Microscopy, Thornwood, NY) or into an HB501 field-emission scanning transmission electron microscope (STEM) (VG Instruments, Beverly, MA) for imaging and analysis. In both instruments, sections were freeze-dried at approximately −110°C and recooled to less than −160°C.

The National Institutes of Health STEM, as well as instrumentation and techniques for cryotransfer, freeze-drying, dark-field imaging and EDX analysis, have been described previously (Leapman and Andrews, 1991; Buchanan et al., 1993). Each EDX analysis was 100 sec at ~4 nA probe current rastered over a 20 × 20 nm area; doses were therefore >10^8 e/nm². We avoid recording spectra from small ER cisterns that are not wholly contained within the section thickness; if such spectra were inadvertently acquired, however, the calculated Ca content would underestimate the ER Ca content. Spectra were recorded at −160°C or below. Data were processed and quantified by established procedures (Shuman et al., 1976; Hall and Gupta, 1983; Kitazawa et al., 1983; Buchanan et al., 1993) using the program DeskTop Spectrum Analyzer for the Macintosh (C. E. Fiori, C. R. Swyt, and R. L. Myklebust, Office of Standard Reference Data, National Institute of Standards and Technology, Gaithersburg, MD). Concentrations are given in millimoles per kilogram of dry weight because the Hall quantification procedure (Hall and Gupta, 1983) provides these data directly. Concentrations in millimoles per liter of original wet volume, which are more intuitively useful in physiology, can be estimated by multiplying dry weight concentrations by the dry mass fraction of analyzed organelles; typical values are 15, 25, and 40% dry mass for cytoplasm, ER, and mitochondria, respectively (Buchanan et al., 1993). It is further possible to convert values to mM, i.e., millimoles per liter of cell water, by dividing by the water fraction of each compartment, but this is not appropriate for total Ca measurements, because most of the Ca is not in solution.

The mean Ca concentrations of the apparently normally distributed low-Ca populations seen in Figure 5 were estimated by least-squares fitting of Gaussians. Mean concentrations and uncertainties derived by curve fitting are reasonable for the statistical and biological variability expected from EDX analysis; curve fitting has the additional merit of accounting for the negative concentration values, which occur because of statistical fluctuations in the subtraction of a fitted background when true Ca x-ray counts are very low (Kitazawa et al., 1983). The minimum detectable concentration can be taken as twice the estimated analytical uncertainty, which is typically 2–4 mmol/kg dry weight for a single analysis under our conditions (Andrews et al., 1994); the SEM for pooled analyses, however, is much lower (e.g., Table 1). Measured concentrations smaller than twice their corresponding SEMs, including zero and negative values, are equivalent to "not detected."

RESULTS

Structural characterization of organelles and compartments in CA3 dendrites

Proximal apical dendrites of CA3 pyramidal neurons within st. lucidum (<100 μm from cell bodies) of rapidly frozen, freeze-substituted hippocampal slice cultures (Pozzo-Miller and Landis, 1993) displayed the characteristic complement of membrane-bound organelles described in more conventional preparations of nervous tissue (Peters et al., 1991) (Fig. 1). Most dendritic branches contained abundant mitochondria, usually elongated and oriented along the longitudinal axis of the dendrite. The ER network consisted of pleomorphic cisterns and tubules of variable dimensions coursing among longitudinal arrays of microtubules; frequently, cisterns ran in close proximity to the plasma membrane. The number and size of ER cisterns and mitochondria varied between dendritic branches (Fig. 1, compare *A, B*). However, the volume-fractions occupied by these organelles appeared on average similar to those found in hippocampal CA1 pyramidal and Purkinje cell dendrites, which in the case of the ER is ~10% of dendritic volume (Martone et al., 1993; Spacek and Harris, 1997). Although Golgi cisterns have been observed in dendrites near the cell body (Peters et al., 1991; Krijnse-Locker et al., 1995), they were rarely, if ever, encountered in the more distal portions selected for the present study.

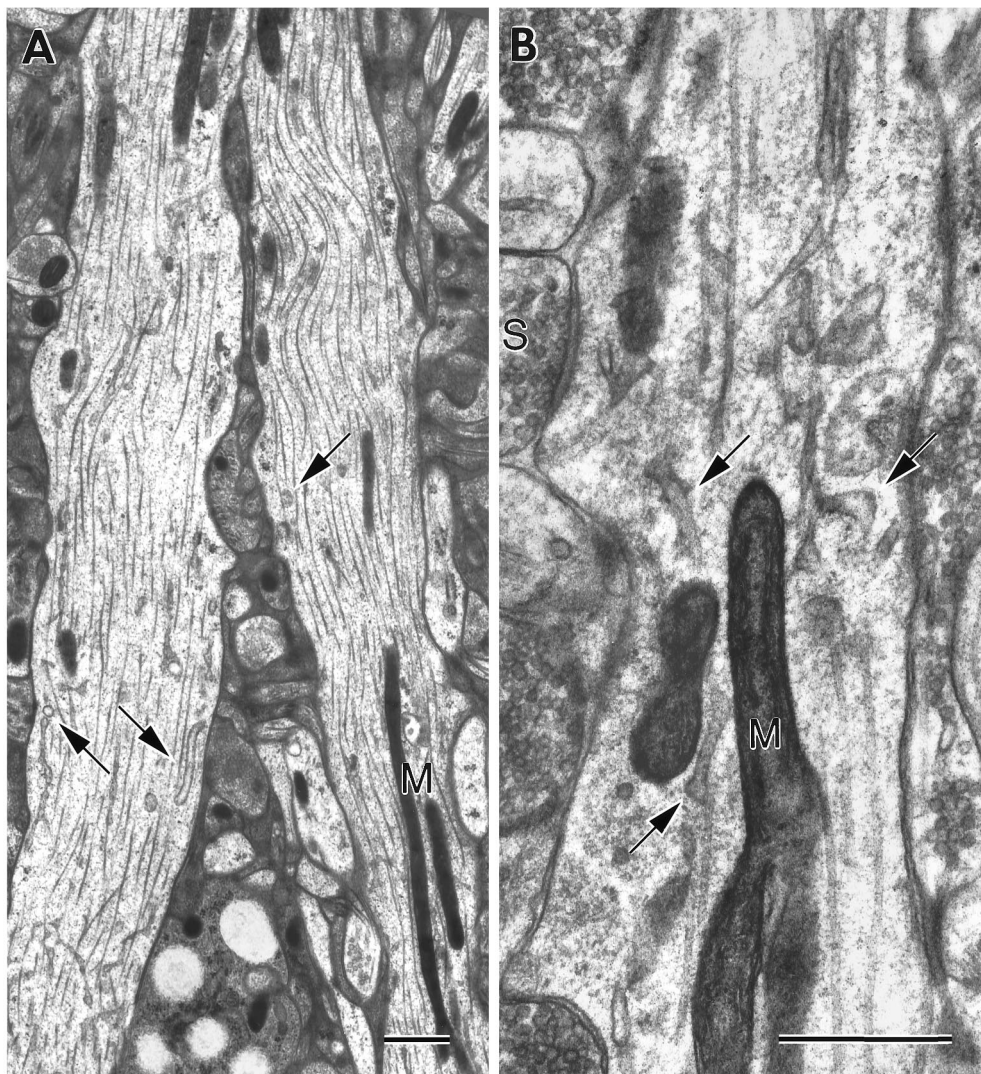All of the the major dendritic compartments found in freeze-

Figure 1. Subcellular organization of CA3 hippocampal dendrites in slice culture. *A, B,* Transmission electron micrographs of dendrites in CA3 st. lucidum from thin sections of rapidly frozen, freeze-substituted slice cultures of hippocampus. These fields illustrate proximal apical dendrites in which mitochondria (*M*) and cisterns of ER (*arrows*) are essentially the only intracellular organelles; the remaining dendritic volume is occupied by microtubule-rich cytoplasm. The general organization is similar in both larger dendrites with sparse organelles (*A*) and in smaller dendrites with a higher density of ER and mitochondria (*B*). Synapses (*S*) directly on the dendritic shaft are evident (*B*). The typical pleomorphic appearance of smooth-membrane cisterns and tubules was consistent with the organization of dendritic ER as a physically interconnected network (Martone et al., 1993; Terasaki et al., 1994). All such cisterns and tubules were defined as ER, because there was no structural basis for making finer distinctions, even though it was recognized that the ER compartment so defined would be functionally heterogeneous (Henzi and MacDermott, 1992; Pozzan et al., 1994). Scale bars, 0.5 μm.

substituted, plastic-embedded cultures, as just described, can also be unambiguously identified in *en face* ultrathin (80 nm effective thickness) cryosections from the superficial 5–20 μm of unfixed, unstained, rapidly frozen slice cultures (Fig. 2). Elemental analysis was performed on apical dendrites within CA3 st. lucidum which were considered as divided into three compartments: ER (including both cisterns and tubules), mitochondria, and a third compartment, referred to as cytoplasm, that consisted mainly of soluble proteins and the cytoskeleton. The justification for this simplified view of dendritic structure lies in the fact that these three compartments include all the structures likely to be involved in dendritic Ca^{2+} homeostasis, even while encompassing >95% of the total volume of the dendrite. Thus, the intrusion of unaccounted organelles, e.g., multivesicular bodies or Golgi cisterns, would represent only a minor contribution and not significantly affect the conclusions of the present study.

Basal elemental concentrations in dendritic compartments

Cryosections of rapidly frozen tissue were prepared from unstimulated control slices incubated in normal ACSF and also from control slices after incubation in 5 μM TTX for 15–30 min to block spontaneous synaptic activity. EDX analysis of both preparations revealed that the concentrations of total Ca, as well as of

other elements, in the three target compartments of CA3 apical dendrites (Table 1) were comparable to basal concentrations in other excitable and nonexcitable cells (Somlyo et al., 1977, 1985; Andrews et al., 1988). The mean concentration of Ca within dendritic ER was 5.1 $\pm$ 1.1 mmol/kg dry weight (mean $\pm$ SEM; Table 1), although, as discussed below, this morphologically identified set of ER consists of at least two functionally distinct populations that, under basal conditions, coincidentally display similar low Ca concentrations. This value corresponds to ~1.3 mmol/l hydrated cell volume. (In general, the values for Ca concentrations within ER, given in mmoles per kilogram of dry weight throughout the text, can be converted to millimoles per liter of cell volume by multiplying by 0.25; see Materials and Methods for assumptions and calculations, as well as conversion factors for other compartments).

Dendritic endoplasmic reticulum is the major calcium sequestration organelle after synaptic activity

Knowing the basal Ca levels, we next determined which dendritic organelles showed changes in total Ca concentration after afferent stimulation. For these experiments, EPSPs in CA3 st. lucidum were evoked by extracellular stimulation of granule cells in dentate gyrus st. granulosum or mossy fiber tracks in CA3 st. lucidum (Fig. 3*A,B*). After establishing a stimulus intensity that evoked
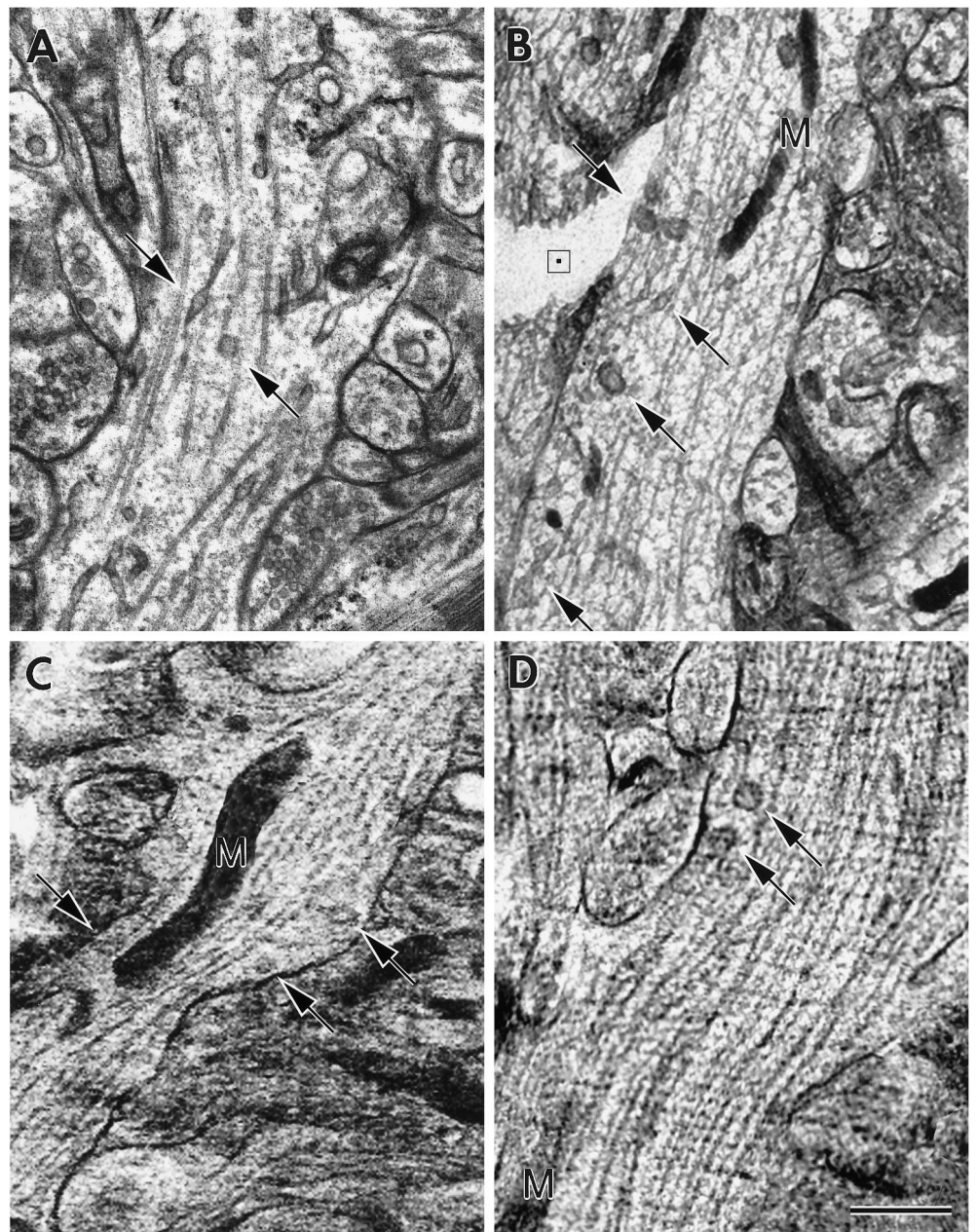
Figure 2. Dendritic structure in cryosections. *A–D*, Electron micrographs of dendrites in CA3 st. lucidum from rapidly frozen slice cultures of hippocampus. Micrographs of unstained, freeze-dried, ultrathin *en face* cryosections from the superficial 5–20 μm of slices (*B–D*) were digitally recorded (1024 × 1024 pixels) at approximately −170°C and low electron dose (~10^3 e nm^{-2}), either in the zero loss mode of an energy-filtering TEM equipped with a slow-scan CCD camera or in STEM elastic dark-field mode. Structural organization and preservation in cryosections (*B–D*) allow direct correlation with structures seen in plastic-embedded preparations (*A*). Compartments targeted for EDX analysis, namely, ER (*arrows*), mitochondria (*M*), and microtubule-rich cytoplasm, can be readily identified, whether from well frozen areas of the specimen (*C, D*) or from less well preserved areas (*B*). In fact, visualization of membrane-bound organelles is easier in cryosections from deeper areas of the slice, which exhibit some degree of freezing damage, because aggregation of cytoplasmic material creates a coarser matrix in which organelles stand out. The *small black square* within the *box* in cracked area of cryosection (*B*) indicates size of a typical 20 × 20 nm analysis raster. Scale bar, 0.5 μm.

stable EPSPs, afferent fibers received either a single tetanus (1 sec, 50 Hz; Fig. 3*C*) or four such tetani at 30 sec intervals. Such high-frequency afferent stimulation is sufficient to activate most, if not all, mechanisms of dendritic Ca^{2+} entry, including influx through locally activated low-voltage-gated Ca^{2+} channels (Magee et al., 1995) and NMDA receptors (Perkel et al., 1993; Petrozzino et al., 1995), plus more widespread voltage-gated influx triggered by back-propagating action potentials (Jaffe et al., 1992; Miyakawa et al., 1992; Spruston et al., 1995). In CA3 and CA1 apical dendrites in slice cultures, this stimulation protocol is known to evoke micromolar free Ca^{2+} transients, which decay to approximately prestimulus levels in 20–30 sec (Pozzo-Miller et al., 1993; Petrozzino et al., 1995).

In slices in which the distribution of Ca ions was preserved by rapid freezing 3 min after a single tetanus, i.e., at a time chosen to be well after the decay of free Ca^{2+} transients, the total Ca concentration had increased to >15 mmol/kg dry weight in 40%

of dendritic ER cisterns; this population of cisterns had a mean of 41 ± 7 mmol/kg (Fig. 4). Because Ca concentrations >15 mmol/kg dry weight clearly indicate a significant increase in Ca content, we propose that the population of responsive cisterns showing such increases represents a Ca sequestering component of the ER. In contrast to the large increase in Ca within some ER cisterns, there was no change in the Ca content of dendritic mitochondria, and only a small, statistically insignificant increase in cytoplasmic Ca after a single tetanus (Fig. 4). There was no significant change in any other measured element in any cellular compartment (Table 1).

Three minutes after four tetani at 30 sec intervals, total Ca increased to a mean of 72 ± 8 mmol/kg in the slightly larger (45%) subset of ER cisterns that exceeded 15 mmol/kg (Fig. 4). The Ca concentrations achieved in the most avidly accumulating cisterns approached, and even occasionally exceeded, 100 mmol/kg, a level otherwise found only in the sarcoplasmic reticulum of

Table 1. Elemental concentrations in cellular compartments of hippocampal CA3 dendrites

	n	Na	K	Ca
		(mmol/kg dry weight)		
Endoplasmic reticulum[a]				
Control ± TTX	56	76 ± 7	571 ± 20	5.1 ± 1.1
Single train	68	91 ± 8	626 ± 24	17.8 ± 3.5*
4 Trains	68	181 ± 13*	505 ± 14	35.5 ± 5.4*
4 Trains + TTX	39	152 ± 11*,**	683 ± 39	6.2 ± 2.3**
4 Trains + recovery	47	41 ± 5**	509 ± 21	8.0 ± 1.5**
4 Trains + thapsigargin	54	101 ± 14**	497 ± 18	5.0 ± 0.8**
Mitochondria				
Control ± TTX	22	32 ± 4	286 ± 12	0.3 ± 1.0***
Single train	8	17 ± 4	239 ± 22	1.8 ± 2.0***
4 Trains	21	62 ± 7*	288 ± 14	1.3 ± 0.6
4 Trains + TTX	12	44 ± 7	267 ± 12	−1.3 ± 0.9***
4 Trains + recovery	32	19 ± 3**	232 ± 11	0.6 ± 0.8***
4 Trains + thapsigargin	29	63 ± 10*	258 ± 14	
Matrices	13			3.7 ± 1.4*,**
Inclusions	16			165 ± 94
Cytoplasm				
Control ± TTX	18	77 ± 16	854 ± 61	0.7 ± 1.1***
Single train	16	72 ± 12	990 ± 88	3.5 ± 3.4***
4 Trains	63	266 ± 28*	772 ± 30	4.2 ± 0.9*
4 Trains + TTX	14	147 ± 16*,**	854 ± 93	1.2 ± 1.5**,***
4 Trains + recovery	18	70 ± 17**	864 ± 97	0.4 ± 1.9**,***
4 Trains + thapsigargin	28	179 ± 39*,**	599 ± 35*,**	1.8 ± 1.6***

Data are given as mean ± SEM, where column *n* is the number of compartments analyzed; the number of ER analyzed ranged from three to seven per dendrite (fewer for other compartments). There were at least two slices for each condition, with dendrites distributed as follows: control ± TTX, 21 dendrites; single train, 25; 4 trains, 31; 4 trains + TTX, 9; 4 trains + recovery, 15; 4 trains + thapsigargin, 28. SE and *n* values are based on compartmental analyses, because a statistical evaluation of the data indicated that dendrite-to-dendrite and slice-to-slice variabilities were small compared with compartment-to-compartment variability. The quantification procedure provides concentrations in units of millimoles per kilogram of dry weight; conversion to millimoles per liter of hydrated cell volume is described in Materials and Methods.

[a] Morphologically defined ER consisted of multiple populations with differing Ca uptake capacities, as discussed in the text and illustrated in Figure 5. Therefore, mean concentrations reported in this table are not necessarily derived from normal distributions. Large SEs result when the underlying populations are different, for example, ER Ca concentrations after one or four stimulus trains.

* Significantly *higher* than corresponding values from resting control cultures, except cytoplasmic K^+ after four trains in the presence of thapsigargin, which is lower; *t* test, $p < 0.05$.

** Significantly *lower* than corresponding values from cultures subjected to four stimulus trains, except Ca in mitochondrial matrices after four trains in the presence of thapsigargin, which is higher; *t* test, $p < 0.05$.

*** Not significantly different from zero. However, the data are given to indicate the errors of Ca analyses, which in this case are mainly limited by counting times. Negative values, reflecting statistical fluctuations, sometimes occur for populations that are not significantly different from zero.

skeletal muscle (Somlyo et al., 1977). Again, there was no increase in mitochondrial Ca and only a modest but statistically significant rise in cytoplasmic total Ca. The latter result suggests that this mode of ER sequestration is proportional to the cytoplasmic Ca load, as would be expected if saturation of cytoplasmic buffers is a prerequisite to ER accumulation. Among the other elements, only Na^+ showed significant increases (Table 1). Increases in Na^+ content (relative to resting cultures) also occurred in other experiments using the four-train protocol (see below), and presumably reflect a combination of opening Na^+ channels by membrane depolarization (Jaffe et al., 1992), permeation through AMPA/kainate subtype of glutamate receptors, and enhanced activity of the Na^+–Ca^{2+} exchanger (Blaustein, 1988; Kiedrowski et al., 1994).

After four tetani at 30 sec intervals in the presence of 5 μM TTX, no Ca uptake occurred in any cellular compartment, including the ER (Table 1, Fig. 4). The TTX dependence of Ca uptake suggests that the observed Ca sequestration in ER is a consequence of synaptic activity. The Na^+ elevation observed after four-train stimulation was significantly reduced in cultures given four stimulus trains in the presence of 5 μM TTX (Table 1). A residual increase in cellular Na^+ after high-frequency stimulation in TTX (compared with resting cultures) may reflect the activity of TTX-insensitive Na^+ channels (Yoshida, 1994).

Calcium sequestration only occurs in a subset of dendritic endoplasmic reticulum

Analysis of the frequency distributions of ER Ca content under different conditions of stimulation provided evidence for at least two subpopulations of ER cisterns, only one of which was involved in Ca sequestration. In resting dendrites and in dendrites stimulated in the presence of TTX, the distributions of Ca content for all cisterns, which presumably included both responsive and nonresponsive organelles, are well described as normal populations with means of 3.5 ± 0.7 and 1.7 ± 0.9 mmol/kg, respectively (Fig. 5A,D). In contrast, the distribution of Ca con-
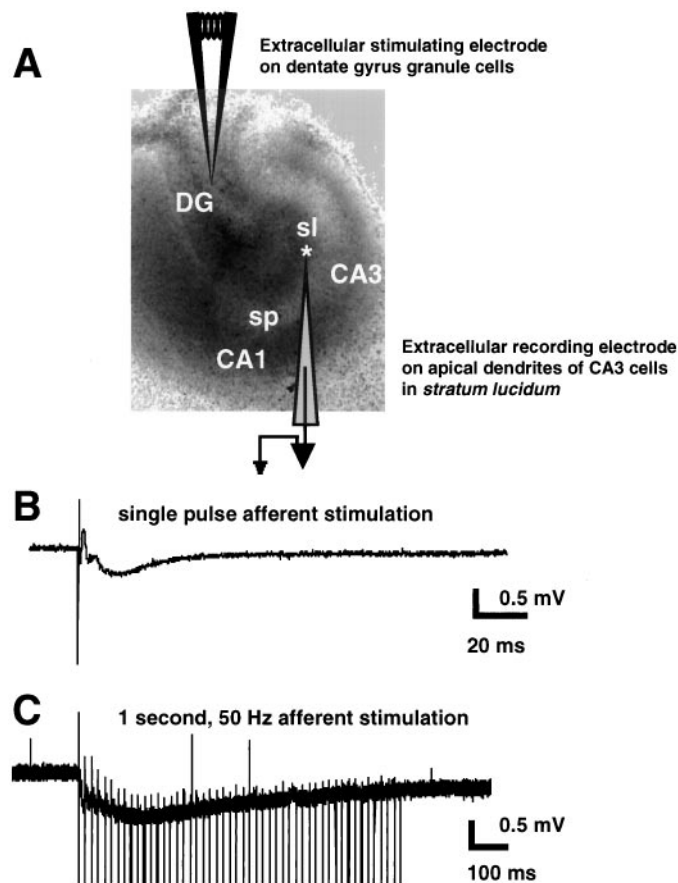
Figure 3. Stimulation and recording of EPSPs in hippocampal slice cultures. *A*, Infrared bright-field image of 9 d *in vitro* hippocampal slice culture showing the placement of recording electrode in CA3 st. lucidum (*asterisk*) and stimulating electrode in dentate granule cells. *B*, Postsynaptic response to a single afferent pulse to dentate granule cells (average of 10 traces). *C*, Postsynaptic response to a 1 sec, 50 Hz train of afferent pulses to dentate granule cells (single trace; stimulus artifacts were trimmed for illustration). *sl*, St. lucidum; *sp*, st. pyramidale.

tent after a single tetanus is multimodal (Fig. 5*B*). Nevertheless, the distribution of Ca concentrations in the ~60% of nonresponsive cisterns that did not exceed the 15 mmol/kg threshold still fits a normal distribution with a mean, 3.7 ± 0.7 mmol/kg, indistinguishable from those of unstimulated dendritic ER (Fig. 5, compare *A, D* with *B*).

As with the single afferent train, there was also a residual pool of nonresponsive ER cisterns after four tetani (Fig. 5*C*). The size of this pool, 55% of all cisterns, was reduced only slightly by the recruitment of cisterns into the responsive pool, even though the Ca content of responsive cisterns was dramatically increased (Fig. 4; also compare *black bars* in Fig. 5*B,C*); this further suggests, in view of the significantly higher Ca load after four trains, that nonresponsive cisterns lack the capacity to accumulate or store Ca. No spatial or structural differences between accumulating and nonaccumulating cisterns were apparent. It was noted that the two types of cisterns, although apparently randomly distributed within dendrites, frequently occurred in close proximity (Fig. 6).

Calcium sequestration in endoplasmic reticulum is reversible and dependent on a Ca^{2+}–ATPase pump

Additional experiments further characterized the Ca^{2+}-buffering organelles by demonstrating reversibility and identify-
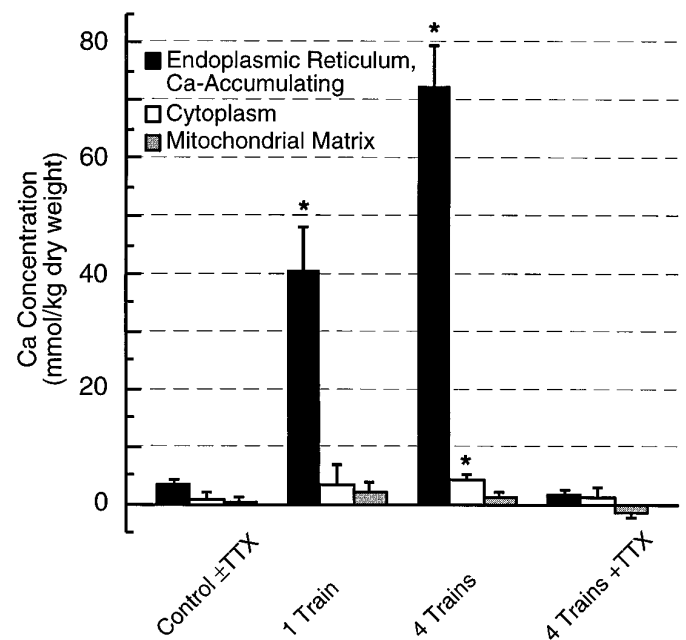

Figure 4. Calcium sequestration in dendritic ER after synaptic activity. Histograms comparing Ca concentrations within dendritic organelles 3 min after afferent stimulation reveal that Ca was sequestered predominantly in a responsive population of ER (*1 Train, 4 Trains*). Uptake into ER was graded with increased number of afferent trains (*1 Train* vs *4 Trains*) and inhibited by blocking action potential-mediated synaptic transmission (*4 Trains+TTX*). In contrast, elemental Ca concentrations in dendritic compartments of control slices rapidly frozen with no afferent stimulation, either in normal ACSF or in the presence of TTX, were uniformly low (*Control±TTX*). (Slices frozen untreated and after incubation in TTX were indistinguishable and therefore were pooled.) Cytoplasmic Ca was slightly but significantly elevated after four afferent stimulus trains; no other differences are statistically significant (*) at $p < 0.05$ level.

ing the uptake mechanism. In slices rapidly frozen after a recovery period of 15–30 min after high-frequency stimulation, Ca distributions, both between compartments and within ER, were indistinguishable from those of resting control slices (Figs. 5*E*, 7). This indicates that the ER can unload Ca^{2+}, presumably via a leak or by spontaneous Ca^{2+} release. The Ca sequestration activity of the ER was abolished by incubation in 10 μM thapsigargin, an inhibitor of the ER Ca^{2+}–ATPase (Figs. 5*F*, 7). Although thapsigargin at these concentrations is known to affect voltage-gated Ca^{2+} channels (Shmigol et al., 1995), blockade of voltage-gated Ca^{2+} influx does not appear to be the major effect here, because a large component of Ca sequestration was diverted to dendritic mitochondria. Thus, a small but significant increase, to 3.7 ± 1.4 mmol/kg, was observed in the mean Ca content of mitochondrial matrices, whereas the number of mitochondria that exhibited large focal increases in Ca was dramatically increased (Fig. 7, Table 1). These sites of elevated Ca generally appeared as dense matrix inclusions with highly variable Ca contents, frequently well in excess of 100 mmol/kg dry weight.

DISCUSSION

This study provides the first direct correlation—at the electron microscopic level—of the concentrations of total Ca within identified subcellular compartments with the physiological activity of central vertebrate neurons. Our approach depended on combin-
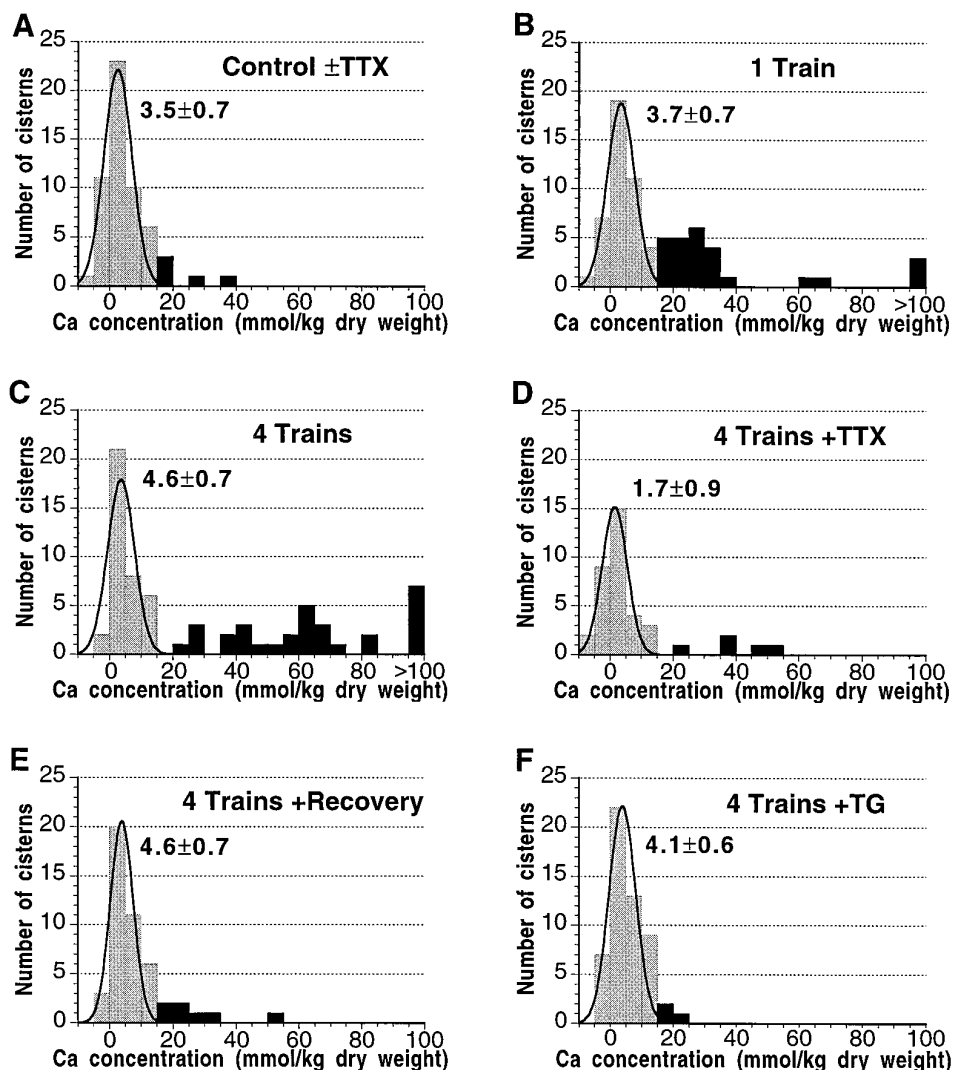
Figure 5. Calcium sequestration in a subpopulation of dendritic ER. *A–F*, Frequency distributions of Ca concentrations within ER cisterns after different stimulation protocols reveal that Ca^{2+} sequestration is limited to a subset of ER cisterns. The multimodal nature of these distributions was evident under conditions (*B, C*) in which increased Ca^{2+} influx led to the separation of the Ca-accumulating population (*black bars*) from a nonresponsive population (*gray bars*). Thus, in dendrites stimulated with one (*B*) and four (*C*) afferent trains, 40 and 45% of the cisterns, respectively, accumulated enough Ca to exceed the arbitrary but conservative cutoff of 15 mmol/kg dry weight. The concentrations reached by the Ca-accumulating cisterns were nonuniformly distributed; those achieving extraordinary levels >100 mmol/kg have been pooled at the *right edges* of *B* and *C*. The mean Ca concentrations of the residual nonresponsive populations, as estimated by least-squares fitting of Gaussians (*solid curves* with mean ± SEM) were not significantly different one from the other, nor were they different from the mean Ca concentrations for the four nonaccumulating conditions (*A, D–F*). In the latter cases, Ca distributions of the low-Ca cisterns (*gray bars*) are probably also multimodal but (apart from a few outliers) appear normally distributed, because the population means are similar and cannot be distinguished.

ing the physiological control available in hippocampal slices, the ability of rapid freezing (Van Harreveld and Crowell, 1964) to immobilize diffusible ions in <2 msec (Heuser et al., 1979), and the high spatial resolution of modern quantitative EDX microanalysis (Leapman and Andrews, 1991; Buchanan et al., 1993; Andrews et al., 1994). The latter is a well established technique for quantitatively measuring total element concentrations with submicrometer spatial resolution. Furthermore, because it detects the large fraction of Ca (>99.9% in the case of the cytoplasm) that constitutes the bound Ca pool, it provides valuable complementary information to the free Ca^{2+} measurements obtained by optical methods using Ca^{2+}-sensitive fluorescent dyes in living slice preparations.

Calcium sequestration by dendritic endoplasmic reticulum

The results demonstrate that the Ca load associated with dendritic Ca^{2+} transients persists for many minutes after the decay of these transients, and that in this time frame and in terms of achievable Ca concentration, the ER is the dominant sequestering compartment. When viewed in terms of total Ca-binding capacity, the ER and cytoplasmic buffers appear to be approximately equal, mainly because the volume fraction of the cytoplas-

mic compartment is so much larger that a sixfold increase in total cytoplasmic Ca, as observed after four tetani, is roughly equivalent to the concomitant 20-fold increase in the ER. Nevertheless, the Ca load attained by some ER cisterns is extraordinary, reaching levels (>100 mmol/kg dry weight) that are unknown outside of the sarcoplasmic reticulum of skeletal muscle (Somlyo et al., 1977). Even so, this large accumulation is apparently within the range of normal physiological activity for these dendrites, as indicated by the modest, parallel elevation of cytoplasmic total Ca in comparison with unstimulated dendrites, and by the reversibility of ER and cytoplasmic Ca sequestration when slices were allowed a recovery period. This recovery presumably reflects the action of slow-acting plasma membrane pumps and exchangers returning intracellular Ca—including ER Ca that unloads by equilibration between ER and cytosolic free Ca^{2+}—to resting levels (also see Pozzo-Miller et al., 1996). Because the recovery phase has a lifetime of 15–30 min, the total Ca content within ER stores available for release by IP_3 and/or ryanodine receptor signaling pathways during this time could serve as a memory trace of previous strong neuronal activity. Ca^{2+} extrusion, and not just redistribution, is most likely occurring during the recovery period, because EDX analysis records a decrease in total Ca content integrated over all cellular compartments.
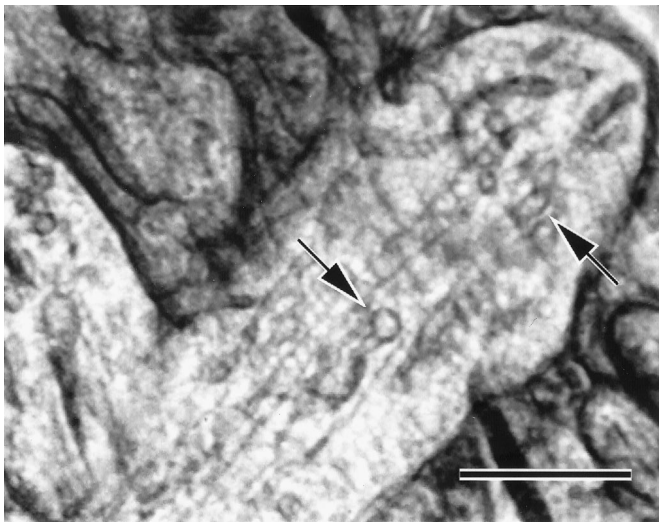
Figure 6. Ca-accumulating and nonaccumulating cisterns of ER. Electron micrograph of a cryosection showing a representative dendrite of CA3 st. lucidum from a rapidly frozen slice culture of hippocampus, recorded as described in legend to Figure 2. This culture was frozen 3 min after the last of four afferent trains. The field illustrates a pair of ER cisterns (*arrows*) that are structurally and spatially similar, as far as can be determined in cryosections. Nevertheless, the *bottom left* member of the pair had a total Ca content exceeding 70 mmol/kg dry weight, while the *top right* cistern contained only 5 mmol/kg. Although the low-calcium cistern is apparently closer to the plasma membrane in this dendrite, this is not reliably the case. Scale bar, 0.5 μm.

Functional heterogeneity and molecular identity of Ca-sequestering cisterns

Under conditions of Ca^{2+} entry, we observed a clear distinction between a non-normally distributed, Ca-sequestering pool of ER and a normally distributed, nonresponsive pool. The invariant Ca content of the nonresponsive pool under conditions that induce large changes in both free and total Ca indicates that this pool is incapable of Ca accumulation or storage. It further implies that avid Ca accumulation in responsive cisterns occurs because this is a specific property of that subpopulation and not merely a consequence of variability in sampling or in dendritic activity or geometry. The heterogeneous response in stimulated dendrites cannot be explained by gradients or heterogeneities in free Ca^{2+} concentrations, because responsive and nonresponsive ER cisterns were intermixed and similarly situated within the same dendritic segments. These results add additional support to the emerging concept (Henzi and MacDermott, 1992; Pozzan et al., 1994; Golovina and Blaustein, 1997; Korkotian and Segal, 1997) that the ER consists of several subtypes of spatially and functionally distinct membrane-bound organelles, some fraction of which are specialized to play a critical role in Ca^{2+} regulation.

An extensive literature describes the distribution of various membrane and luminal proteins regulating Ca^{2+} homeostasis in dendrites of different brain regions and in different species (for review, see Henzi and MacDermott, 1992; Pozzan et al., 1994). In the case of rodent hippocampal pyramidal dendrites, the present observation of thapsigargin-sensitive Ca sequestration into ER cisterns implies the presence of a SERCA pump, while the presence of IP$_3$- and ryanodine-sensitive release channels has been shown immunocytochemically (Sharp et al., 1993), and by optical imaging of Ca^{2+}-sensitive dyes (Seymour-Laurent and Barish, 1995; Pozzo-Miller et al., 1996; Garaschuk et al., 1997; Korkotian and Segal, 1997). Our finding that approximately half of the
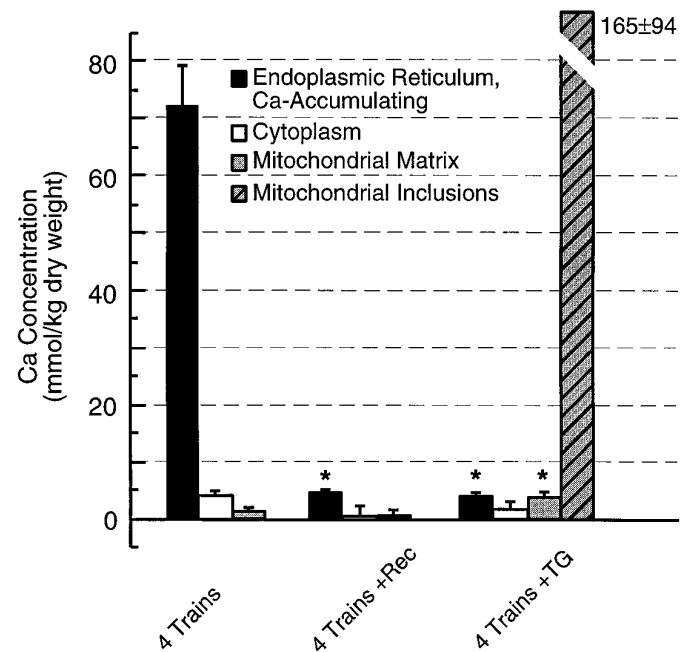

Figure 7. Reversibility and inhibition of ER calcium sequestration. Comparison of Ca concentrations within dendritic organelles at 3 min (*4 Trains*) and 15 min (*4 Trains+Rec*) after four afferent stimulation trains reveals that Ca^{2+} uptake into ER was reversible. Ca^{2+} uptake into ER was dependent on a thapsigargin-sensitive Ca^{2+}–ATPase pump (*4 Trains+TG*). Ca accumulated within mitochondria, either diffusely within the matrix (*gray bar*) or in the form of small inclusions (*hatched bar*), only when ER Ca^{2+}–ATPase pumps were inhibited; under these conditions there were no large increases in the Ca content of any other organelle. *Asterisks* indicate statistical significance (*p* <0.05) relative to *4 Trains* stimulation.

smooth membrane organelles structurally identified as ER appear to function as Ca^{2+} sinks or sources is consistent, in light of recent observations of others (Golovina and Blaustein, 1997), with the tentative identification of dendritic Ca sequestration organelles as identical to Ca^{2+} release organelles, sequestration being an alternative functional response to a different physiological demand. The remaining nonresponsive ER would then consist of molecularly different cisterns involved in other functions, such as synthesis and transport of cell components.

The role of mitochondrial Ca sequestration

The complete dominance of ER Ca sequestration over mitochondrial uptake at 3 min after stimulation provides no support for mitochondrial involvement at this rather late time but does not necessarily contradict recent studies demonstrating a significant role for mitochondrial Ca^{2+} buffering at early times after cytoplasmic Ca^{2+} elevation (Herrington et al., 1996; Babcock et al., 1997). The fact that mitochondrial uptake is transient and followed by extrusion within 1 min after Ca^{2+} elevation (Herrington et al., 1996; Padua et al., 1996)—a process that is much faster than release from the ER—is in good agreement with our measurements of low mitochondrial Ca content 3 min after stimulation. Nonetheless, the elevated levels of mitochondrial Ca observed at 3 min after synaptic stimulation in the presence of an ER Ca^{2+}-ATPase inhibitor show that dendritic mitochondria are capable of accumulating and retaining Ca. Additionally, preliminary results indicate that when hippocampal slices were rapidly frozen 30 sec after a single tetanus, i.e., just after termination of the free dendritic Ca^{2+} transient (Pozzo-Miller et al., 1993;

Petrozzino et al., 1995), significant Ca accumulation occurred in both mitochondria and ER cisterns (Pivovarova et al., 1997). Taken together, these results indicate that mitochondria may well participate in dendritic Ca^{2+} clearance when their "set point" (Carafoli, 1987) for cytoplasmic Ca^{2+} concentration has been exceeded during the seconds after synaptic activity but will retain Ca at later times only in the absence of a functional ER sequestration mechanism. Considering that results from several new (Markram et al., 1995; Budd and Nicholls, 1996), as well as earlier (Somlyo et al., 1985) studies argue against significant mitochondrial participation under other physiological conditions, more work will be necessary to understand the comparative importance of and interplay between these two organelles in dendritic Ca^{2+} buffering.

Methodological considerations

Studies such as this one have only recently become feasible, thanks to technical advances in the development of stable organotypic slice cultures of hippocampus (Stoppini et al., 1991; Pozzo-Miller et al., 1993), as well as methodological advances in biological EDX microanalysis (Buchanan et al., 1993; Andrews et al., 1994). Organotypic slice cultures of deep brain structures offer the advantage of an intact and living surface that can be studied optically and electrophysiologically and subsequently directly frozen using cold metal block techniques (Pozzo-Miller and Landis, 1993; Pozzo-Miller et al., 1993). Because neuronal cell bodies and processes, including axons, dendrites, and synapses, are present within 5–20 μm of the exposed surface of such slices (L. D. Pozzo-Miller, T. S. Reese, and S. B. Andrews, unpublished observations), these components are structurally well preserved (Figs. 1, 2) and—most importantly for this study—also maintain on a millisecond time scale (Heuser et al., 1979) their native distributions of intracellular diffusible ions (Somlyo et al., 1977).

These slice cultures are also well suited for *en face* cryosectioning, which, using newer sectioning techniques (Michel et al., 1992; Buchanan et al., 1993) produces uniform, truly ultrathin cryosections in which even small organelles such as cisterns of ER are unambiguously recognizable (Fig. 2). After freeze-drying, these cryosections are suitable for EDX analysis, which is the principal established method for obtaining direct, quantitative measurements of the total concentrations of Ca, as well as of several other physiologically important chemical elements in parallel, within identified subcellular compartments. It is important to emphasize that over the past decade there have been major technical and instrumental advances in biological EDX analysis (summarized by Buchanan et al., 1993; Andrews et al., 1994). These advances have largely eliminated the problems that plagued many early attempts at biological microanalysis using immature techniques and instruments. Claims for the performance of modern EDX analysis are now well justified (Leapman and Andrews, 1991; Buchanan et al., 1993), with a demonstrated sensitivity of <50 atoms of Ca in analytical volumes smaller than $20 \times 20 \times 60$ nm (Andrews et al., 1994; Shi et al., 1996).

Conclusions

Ca sequestration by ER possesses several of the characteristics expected of an intracellular Ca^{2+} buffering system: (1) it is graded and dependent on neuronal activity; (2) it is reversible, even in the extreme case of repetitive high-frequency stimulus trains; and (3) it is dependent on a SERCA pump, implying a molecular similarity to, even possibly an identity with, IP_3- and/or ryanodine-sensitive Ca^{2+} release organelles. Taken together,

these results directly demonstrate that in CA3 dendrites specific cisterns of ER constitute the major subcellular compartment responsible for Ca sequestration in the minutes after neuronal activity.

REFERENCES

Alford S, Frenguelly BG, Schofield JG, Collingridge GL (1993) Characterization of Ca^{2+} signals induced in hippocampal CA1 neurones by the synaptic activation of NMDA receptors. J Physiol (Lond) 469:693–716.

Andrews SB, Leapman RD, Landis DMD, Reese TS (1988) Activity-dependent accumulation of calcium in Purkinje cell dendritic spines. Proc Natl Acad Sci USA 85:1682–1685.

Andrews SB, Buchanan RA, Leapman RD (1994) Quantitative dark-field mass analysis of ultrathin cryosections in the field-emission STEM. Scanning Microsc Suppl 8:13–24.

Babcock DF, Herrington J, Goodwin PC, Park YB, Hille B (1997) Mitochondrial participation in the intracellular Ca^{2+} network. J Cell Biol 136:833–844.

Blaustein MP (1988) Calcium transport and buffering in neurons. Trends Neurosci 11:438–443.

Buchanan RA, Leapman RD, O'Connell MF, Reese TS, Andrews SB (1993) Quantitative scanning transmission electron microscopy of ultrathin cryosections: subcellular organelles in rapidly frozen liver and cerebellar cortex. J Struct Biol 110:244–255.

Budd SL, Nicholls DG (1996) A reevaluation of the role of mitochondria in neuronal Ca^{2+} homeostasis. J Neurochem 66:403–411.

Carafoli E (1987) Intracellular calcium homeostasis. Annu Rev Biochem 56:395–433.

Friel DD, Tsien RW (1994) An FCCP-sensitive Ca^{2+} store in bullfrog sympathetic neurons and its participation in stimulus-evoked changes in $[Ca^{2+}]_i$. J Neurosci 14:4007–4024.

Garaschuk O, Yaari Y, Konnerth A (1997) Release and sequestration of calcium by ryanodine-sensitive stores in rat hippocampal neurones. J Physiol (Lond) 502:13–30.

Golovina VA, Blaustein MP (1997) Spatially and functionally distinct Ca^{2+} stores in sarcoplasmic and endoplasmic reticulum. Science 275:1643–1648.

Hall TA, Gupta BL (1983) The localization and assay of chemical elements by microprobe methods. Q Rev Biophys 16:279–339.

Henkart MP, Reese TS, Brinley Jr FJ (1978) Endoplasmic reticulum sequesters calcium in the squid giant axon. Science 202:1300–1303.

Henzi V, MacDermott AB (1992) Characteristics and function of Ca^{2+}- and inositol 1,4,5-trisphosphate-releasable stores of Ca^{2+} in neurons. Neuroscience 46:251–273.

Herrington J, Park YB, Babcock DF, Hille B (1996) Dominant role of mitochondria in clearance of large Ca^{2+} loads from rat adrenal chromaffin cells. Neuron 16:219–228.

Heuser JE, Reese TS, Dennis MJ, Jan Y, Jan L, Evans L (1979) Synaptic vesicle exocytosis captured by quick freezing and correlated with quantal transmitter release. J Cell Biol 81:275–300.

Jaffe DB, Johnston D, Lasser-Ross N, Lisman JE, Miyakawa H, Ross WN (1992) The spread of Na^+ spikes determines the pattern of dendritic Ca^{2+} entry into hippocampal neurons. Nature 357:244–246.

Kiedrowski L, Brooker G, Costa E, Wroblewski JT (1994) Glutamate impairs neuronal calcium extrusion while reducing sodium gradient. Neuron 12:295–300.

Kitazawa T, Shuman H, Somlyo AP (1983) Quantitative electron probe analysis: problems and solutions. Ultramicroscopy 11:251–261.

Korkotian E, Segal M (1997) Calcium-containing organelles display unique reactivity to chemical stimulation in cultured hippocampal neurons. J Neurosci 17:1670–1682.

Krijnse-Locker J, Parton RG, Fuller SD, Griffiths G, Dotti CG (1995) The organization of the endoplasmic reticulum and the intermediate compartment in cultured rat hippocampal neurons. Mol Biol Cell 6:1315–1332.

Leapman RD, Andrews SB (1991) Analysis of directly frozen macromolecules and tissues in the field-emission STEM. J Microsc (Oxf) 161:3–19.

Llano I, DiPolo R, Marty A (1994) Calcium-induced calcium release in cerebellar Purkinje cells. Neuron 12:663–673.

Magee JC, Christofi G, Miyakawa H, Christie B, Lasser-Ross N, Johnston D (1995) Subthreshold synaptic activation of voltage-gated Ca^{2+}

channels mediates a localized Ca^{2+} influx into the dendrites of hippocampal pyramidal neurons. J Neurophysiol 74:1335–1342.

Markram H, Helm PJ, Sakmann B (1995) Dendritic calcium transients evoked by single back-propagating action potentials in rat neocortical pyramidal neurons. J Physiol (Lond) 485:1–20.

Martone ME, Zhang Y, Simpliciano VM, Carragher BO, Ellisman MH (1993) Three-dimensional visualization of the smooth endoplasmic reticulum in Purkinje cell dendrites. J Neurosci 13:4636–4646.

McGraw CF, Somlyo AV, Blaustein MP (1980) Localization of calcium in presynaptic nerve terminals. An ultrastructural and electron microprobe analysis. J Cell Biol 85:228–241.

Michel M, Gnägi H, Müller M (1992) Diamonds are a cryosectioner's best friend. J Microsc (Oxf) 166:43–56.

Miller RJ (1988) Calcium signalling in neurons. Trends Neurosci 11:415–419.

Miller RJ (1991) The control of neuronal Ca^{2+} homeostasis. Prog Neurobiol 37:255–285.

Miyakawa H, Ross WN, Jaffe D, Callaway JC, Lasser-Ross N, Lisman JE, Johnston D (1992) Synaptically activated increases in Ca^{2+} concentration in hippocampal CA1 pyramidal cells are primarily due to voltage-gated Ca^{2+} channels. Neuron 9:1163–1173.

Padua RA, Campbell C, Thayer SA (1996) Measurement of mitochondrial $[Ca^{2+}]$ in cultured rat neurons transfected with mitochondrial-targeted aequorin. Soc Neurosci Abstr 22:378.

Perkel DJ, Petrozzino JJ, Nicoll RA, Connor JA (1993) The role of Ca^{2+} entry via synaptically activated NMDA receptors in the induction of long-term potentiation. Neuron 11:817–823.

Peters A, Palay SL, Webster HDeF (1991) The fine structure of the nervous system. Neurons and their supporting cells. New York: Oxford.

Petrozzino JJ, Pozzo-Miller LD, Connor JA (1995) Micromolar Ca^{2+} transients in dendritic spines of hippocampal pyramidal neurons in brain slice. Neuron 14:1223–1231.

Pivovarova NB, Pozzo-Miller LD, Leapman RD, O'Connell MF, Reese TS, Andrews SB (1997) Rapid calcium accumulation by endoplasmic reticulum and mitochondria after synaptic activation of CA3 pyramidal dendrites in hippocampal slices. Soc Neurosci Abstr 23:1127.

Pozzan T, Rizzuto R, Volpe P, Meldolesi J (1994) Molecular and cellular physiology of intracellular calcium stores. Physiol Rev 74:595–636.

Pozzo-Miller LD, Landis DMD (1993) Cytoplasmic structure in organotypic cultures of rat hippocampus prepared by rapid freezing and freeze substitution fixation. Synapse 13:195–205.

Pozzo-Miller LD, Petrozzino JJ, Mahanty NK, Connor JA (1993) Optical imaging of cytosolic calcium, electrophysiology, and ultrastructure in pyramidal neurons of organotypic slice cultures from rat hippocampus. NeuroImage 1:109–120.

Pozzo-Miller LD, Petrozzino JJ, Golarai G, Connor JA (1996) Ca^{2+} release from intracellular stores induced by afferent stimulation of pyramidal neurons in hippocampal slice. J Neurophysiol 76:554–562.

Rizzuto R, Brini M, Murgia M, Pozzan T (1993) Microdomains with high Ca^{2+} close to IP$_3$-sensitive channels that are sensed by neighboring mitochondria. Science 262:744–777.

Seymour-Laurent KJ, Barish ME (1995) Inositol 1,4,5-trisphosphate and ryanodine receptor distributions and patterns of acetylcholine- and caffeine-induced calcium release in cultured mouse hippocampal neurons. J Neurosci 15:2592–2608.

Sharp AH, Dawson TM, Ross CA, Fotuhi M, Mourey RJ, Snyder SH (1993) Inositol 1,4,5-trisphosphate receptors: immunohistochemical localization to discrete areas of rat central nervous system. Neuroscience 53:927–942.

Shi S, Sun S, Andrews SB, Leapman RD (1996) Thickness measurement of hydrated and dehydrated cryosections by EELS. Microsc Res Tech 33:241–250.

Shmigol A, Kostyuk P, Verkhratsky A (1995) Dual action of thapsigargin on calcium mobilization in sensory neurons: inhibition of Ca^{2+} uptake by caffeine-sensitive pools and blockade of plasmalemmal Ca^{2+} channels. Neuroscience 65:1109–1118.

Shuman H, Somlyo AV, Somlyo AP (1976) Quantitative electron probe microanalysis of biological thin sections: methods and validity. Ultramicroscopy 1:317–339.

Simpson PB, Challiss RAJ, Nahorski SR (1995) Neuronal Ca^{2+} stores: activation and function. Trends Neurosci 18:299–306.

Somlyo AP, Bond M, Somlyo AV (1985) Calcium content of mitochondria and endoplasmic reticulum in liver frozen rapidly in vivo. Nature 314:622–625.

Somlyo AV, Shuman H, Somlyo AP (1977) Elemental distribution in striated muscle and the effects of hypertonicity. Electron probe analysis of cryo sections. J Cell Biol 74:828–857.

Spacek J, Harris KM (1997) Three-dimensional organization of smooth endoplasmic reticulum in hippocampal CA1 dendrites and dendritic spines of the immature and mature rat. J Neurosci 17:190–203.

Spruston N, Schiller Y, Stuart G, Sakmann B (1995) Activity-dependent action potential invasion and calcium influx into hippocampal CA1 dendrites. Science 268:297–300.

Stoppini L, Buchs L-A, Muller D (1991) A simple method for organotypic cultures of nervous tissue. J Neurosci Methods 37:173–182.

Terasaki M, Slater NT, Fein A, Schmidek A, Reese TS (1994) Continous network of endoplasmic reticulum in cerebellar Purkinje neurons. Proc Natl Acad Sci USA 91:7510–7514.

Tsien RW, Tsien RY (1990) Calcium channels, stores, and oscillations. Annu Rev Cell Biol 6:715–760.

Van Harreveld A, Crowell J (1964) Electron microscopy after rapid freezing on a metal surface and substitution fixation. Anat Rec 149:381–386.

Werth JL, Thayer SA (1994) Mitochondria buffer physiological calcium loads in cultured rat dorsal root ganglion neurons. J Neurosci 14:348–356.

White RJ, Reynolds IJ (1995) Mitochondria and Na^+/Ca^{2+} exchange buffer glutamate-induced calcium loads in cultured cortical neurons. J Neurosci 15:1318–1328.

Yoshida S (1994) Tetrodotoxin-resistant sodium channels. Cell Mol Neurobiol 14:227–244.